Evaluation of the Rate Constant for the S_N2 Reaction $CH_3F + H^- \rightarrow CH_4 + F^-$ in the Gas Phase

Angela Merkel,[†] Zdeněk Havlas,*[‡] and Rudolf Zahradník[§]

Contribution from the Central Institute of Physical Chemistry of Academy of Sciences of GDR, 1199 Berlin-Adlershof, Rudower Chaussee 5, German Democratic Republic, Institute of Organic Chemistry and Biochemistry, Czechoslovak Academy of Sciences, Flemingovo nám. 2, 16610 Prague 6, Czechoslovakia, and J. Heyrovský Institute of Physical Chemistry and Electrochemistry, Czechoslovak Academy of Sciences, Dolejškova 3, 18223 Prague 8, Czechoslovakia. *Received February 19, 1988*

Abstract: Rate constants for the title reaction are calculated within the framework of statistical theories. The input data are taken mainly from recently published ab initio quantum chemical calculations. Comparison with the experimental estimate from flowing afterglow measurements by Tanaka et al. of $k_{obs}^{exp} = 1.5 \times 10^{-11}$ cm^3 s^{-1} shows that, for three of four input data sets, the experimental value can be reproduced with reasonable accuracy. Using two kinetic models, rate constants ranging from 2.1×10^{-12} to 4.5×10^{-11} cm^3 s^{-1} are obtained for these three data sets. Variation of the kinetic model changes the rate constants by up to one order of magnitude. The remaining uncertainties should stimulate further experiments as well as higher level quantum chemical calculations and theoretical treatment of the reaction dynamics.

I. Introduction

In the theoretical investigation of the reactivity and rate constants of polyatomic reactions in the gas phase, bimolecular nucleophilic substitution (S_N2) reactions have attracted considerable attention of theorists for more than 15 years.

In contrast, nucleophilic substitutions are a much older subject in experimental chemistry. Fifty years ago, Hughes and Ingold studied these processes at a sophisticated level (for a comprehensive treatment see the monograph by Ingold[1]). All these studies were performed in solution. An exciting step forward was made in 1970, when an S_N2 process was observed in the gas phase[2] for the first time, initiating a period of investigations in which it was possible to distinguish between the "intrinsic" nucleophilic substitution and solvent effects. The activation energies for a vast number of S_N2 reactions vary typically in the range from 20 to 50 kcal/mol (see e.g., ref 1, 3, and 4). A significant decrease in the activation energies is observed when passing into the gas phase, as predicted[5] in 1959. For example, the reaction of CH_3F with OH^- in solution is slower by 26 orders of magnitude.[6] Gas-phase experiments are performed by two different techniques.

(i) The flowing afterglow technique was used in an early study by Bohme et al.[2] to measure the rate constants of reactions at 25 °C between several ions and CH_3Cl at pressures of 0.2–0.6 Torr. The same technique was used to determine the gas-phase nucleophilicites of the H^-, F^-, OH^-, and NH_2^- anions, where the reaction partners were CH_3F and CH_3Cl with helium as buffer gas.[7,8] Assuming that nucleophilic substitution is a direct, elementary step, activation energies were estimated on the basis of the Eyring theory. It was possible to classify various anion nucleophiles[6] by correlation of the apparent activation energies with the reaction heats.

(ii) Brauman and co-workers utilized pulsed ion cyclotron resonance (ICR) spectroscopy to measure the gas-phase nucleophilic displacement reactions.[9,10] Attempts to understand the wide range of rates for a broad spectrum of reactions in contrast to other ion molecule reactions as well as their negative temperature dependence led to the suggestion that S_N2 reactions proceed on a double-well potential surface.[10] Therefore, instead of a direct process, nucleophilic substitution consists of several elementary steps: the formation and breaking of van der Waals complexes and a unimolecular isomerization step when crossing the barrier. The RRKM theory[11] was used for interpretation of the measured rate constants in terms of features of the potential energy profile, and this made it possible to estimate the barrier heights for several nucleophilic substitution reactions.[2,9,10,12-14] Both the assumption of a double-well energy profile and the kinetic description of the unimolecular elementary steps within the framework of the RRKM theory permitted explanation of all the reaction efficiencies observed. Important conclusions about the nucleophilicity of different anions and leaving group abilities were drawn. These experimental findings were discussed in terms of various rate–equilibrium relationships.[15-17] It was found that the Marcus theory[16] was especially useful for the prediction of barrier heights for a wide variety of asymmetric S_N2 reactions.[13,14]

During the same period, a large number of theoretical investigations were performed, studying parts of the potential energy surface for a given S_N2 reaction employing quantum chemical methods. An excellent review of the literature up to 1981 is given in the thesis by Mitchell,[18] and a recent survey forms part of an article by Basilevsky et al.[19] Most of these studies deal with the elucidation of qualitative aspects of S_N2 reactions in the gas phase. Whereas it was found that semiempirical quantum chemical methods are not appropriate for the investigation of S_N2 reactions,[19] rather simple ab initio quantum chemical methods were

[†] Central Institute of Physical Chemistry of Academy of Sciences of GDR.
[‡] Institute of Organic Chemistry and Biochemistry, Czechoslovak Academy of Sciences.
[§] J. Heyrovský Institute of Physical Chemistry and Electrochemistry, Czechoslovak Academy of Sciences.

(1) Ingold, C. K. *Structure and Mechanism in Organic Chemistry*; Cornell University Press: Ithaca, NY, 1953.
(2) Bohme, D. K.; Young, L. B. *J. Am. Chem. Soc.* **1970**, *92*, 7354.
(3) Shaik, S. S. *Prog. Phys. Chem.* **1985**, *15*, 197.
(4) Albery, W. J.; Kreevoy, M. M. *Adv. Phys. Org. Chem.* **1978**, *16*, 87.
(5) Bathgate, R. H.; Moelwyn-Hughes, E. A. *J. Chem. Soc.* **1959**, 2642.
(6) Tanaka, K.; Mackay, G. I.; Payzant, J. D.; Bohme, D. K. *Can. J. Chem.* **1976**, *54*, 1643.
(7) Young, L. B.; Lee-Ruff, E.; Bohme, D. K. *J. Chem. Soc., Chem. Commun.* **1973**, 35.
(8) Bohme, D. K.; Mackay, G. I.; Payzant, J. D. *J. Am. Chem. Soc.* **1974**, *96*, 4027.
(9) Brauman, J. I.; Olmstead, W. N.; Lieder, C. A. *J. Am. Chem. Soc.* **1974**, *96*, 4030.
(10) Olmstead, W. N.; Brauman, J. I. *J. Am. Chem. Soc.* **1977**, *99*, 4219.
(11) Robinson, P. J.; Holbrook, K. A. *Unimolecular Reactions*; Wiley-Interscience: New York, 1972.
(12) Pellerite, M. J.; Brauman, J. I. *J. Am. Chem. Soc.* **1983**, *105*, 2672.
(13) Chau-Chung Han; Dodd, J. A.; Brauman, J. I. *J. Phys. Chem.* **1986**, *90*, 471.
(14) Dodd, J. A.; Brauman, J. I. *J. Phys. Chem.* **1986**, *90*, 3559.
(15) Hammond, G. S. *J. Am. Chem. Soc.* **1955**, *77*, 334.
(16) Marcus, R. A. *Annu. Rev. Phys. Chem.* **1965**, *15*, 155.
(17) Murdoch, J. R. *J. Am. Chem. Soc.* **1972**, *94*, 4410.
(18) Mitchell, D. J. "Theoretical Aspects of Sn2 Reactions" (Thesis), Queens University, Kingston, Ontario, Canada, 1981.
(19) Basilevsky, M. V.; Koldobsky, S. G.; Tichomirov, V. A. *Usp. Chim.* **1986**, *55*, 1667.

0002-7863/88/1510-8355$01.50/0 © 1988 American Chemical Society

assumed to be sufficient. One of the reasons for these investigations was to explain the stereochemistry of these reactions.[18,20-23] For instance, the principle of structural stability was used for the analysis of S_N2 processes[21] in connection with a study in which all the possible paths were considered.[22] It turned out that, for S_N2 reactions of the $CH_3X + Y^- \rightarrow CH_3Y + X^-$ type, the backside attack is the most favorable. The main part of the calculations concentrated on numerical verification of the validity of rate–equilibrium relationships as they were used for interpretation of the experimental data. Pioneering work in this field was carried out by Mitchell, Wolfe, Shaik, and co-workers.[18,24,25] Very intensive attention was paid to the substituent effect in S_N2 transition states.[24] It was concluded that, rather than the Hammond posulate, the Marcus theory is applicable for the prediction of S_N2 reaction barriers.[24] Numerous calculated values are given in the thesis by Mitchell.[18] Finally, the dominant role of the distortion energy when S_N2 transition states are formed was pointed out. In this connection, related studies on gas-phase deprotonation of carbonic acids and on the kinetic acidities of diastereotopic hydrogens are also worth mentioning.[25]

The effect of α substituents on S_N2 reactions was studied in some detail.[24] We can gather that all these quantum chemical results led to a deeper qualitative insight into the common chemical characteristics of S_N2 reactions, and mainly into the interplay of thermochemical and kinetic forms in the reactions.

Rather rare quantum chemical investigations deal with quantitative predictions of the reaction profile for a particular reaction. This is because accurate energy and structure data for complex polyatomic systems are still difficult to obtain by quantum chemical ab initio methods. Even using the most sophisticated approximations, it is still quite difficult to find a balance description of an entire reaction profile including van der Waals minima and transition states, especially if anions are involved.

To our knowledge, reliable studies of this kind were performed only for the class of reactions $Y^- + CH_3X \rightarrow X^- + CH_3Y$. Dedieu and Veillard were the first to treat classical S_N2 reactions along a double-well energy profile[26] including the correlation energy contributions[27] by means of configuration interaction. They found almost no influence of the correlation energy on the relative reaction profile, in agreement with the general view on the influence of the correlation energy in reactions including only closed-shell reactants and products.

In contrast, the CEPA calculations of Keil and Ahlrichs,[28] carried out in 1976 for a series of the same type of reactions, showed that electron correlation contributes up to ±7 kcal/mol to the activation energies and therefore cannot be neglected.

A further step toward higher level quantum chemical calculations was made by Urban and co-workers using the many-body perturbation theory through the complete fourth order for the reactions $CH_3F + Y^-$ (Y = F, H, OH).[29,30] These studies generally showed a drastic decrease in the barrier height when including the correlation energy contributions. (For a S_N2 reaction with a cationic species, a recent sophisticated study by Raghavachari et al.[31] showed a much smaller influence of the correlation energy than for anionic systems.) Most of these studies suffered from inconsistencies in the number of stationary points along the reaction profile treated, the accuracy of the geometry parameters used, and the level of the vibrational frequency calculations. Complete investigations of the reaction profile including the correlation energy have so far been reported only for the $CH_3F + OH^-$ reaction.[30]

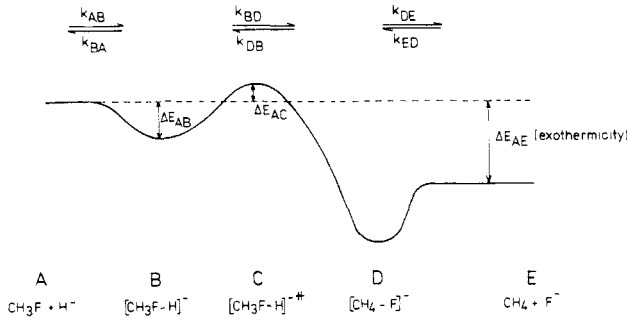

Figure 1. Schematic potential energy profile of the reaction $CH_3F + H^- \rightarrow CH_4 + F^-$.

In an earlier paper[32] we reported our results for the $CH_3F + H^-$ reaction. The geometries of all the stationary points were optimized using the second-order Møller–Plesset perturbation theory; subsequently reaction profiles were estimated employing different quantum chemical methods (second-order Møller–Plesset theory, CEPA, and multiconfiguration SCF methods). It confirmed the findings of Urban and co-workers.[29,30]

No studies are yet available in which the theoretical evaluations were extended to the estimation of the gas-phase rate constants on the basis of a quantum chemically evaluated reaction profile according to the proposals by Olmstead and Brauman.[10] (Černušák et al.[29] have carried out a rate-constant calculation for the $CH_3F + F^-$ reaction using the Eyring theory.[33]) Recently, two-dimensional quantum scattering calculations were performed by Ryaboy and Basilevsky[34] for the $CH_3F + Y^-$ (Y = H, F, OH) reactions on the basis of several ab initio characteristics.

This paper describes the evaluation of the rate constants for the $CH_3F + H^-$ reaction within the framework of statistical theories. The results of the recently reported[32] ab initio quantum chemical calculations were used as input data. The influence of the quality of the quantum chemical data on the evaluated rate constants were discussed and different kinetic models were tested. The resulting reaction efficiencies are compared with the experimental data. Unfortunately, because of the poor leaving group abilities of the fluoride anion (a rather high "intrinsic" barrier), rate constants for reactions with participation of CH_3F could be measured only with the flowing afterglow technique.[6] The detection limit in this technique permits measurements on reactions with an efficiency of less than 10^{-4}, which is about one order of magnitude lower than in the ICR experiments. Therefore, for the reaction under consideration only one experimental value has so far been measured using the flowing afterglow technique.[6]

After a description of the methods employed for the rate constant calculations in section II, the values used for the calculations are summarized in section III and the results are discussed in section IV.

II. Evaluation of Rate Constants

This work was carried out to evaluate the rate constants for the reaction:

(20) Fernandez, A.; Sinanoğlu, O. *Theor. Chim. Acta* **1984**, *56*, 147.
(21) Gremashi, P.; Simonetta, M. *Chem. Phys. Lett.* **1976**, *44*, 70.
(22) Schlegel, H. B.; Mislow, K.; Bernardi, F.; Bottoni, A. *Theor. Chim. Acta* **1977**, *44*, 245.
(23) Ishida, K.; Morokuma, K.; Komornicki, A. J. *J. Chem. Phys.* **1977**, *66*, 245.
(24) Pross, A.; Shaik, S. S. *J. Am. Chem. Soc.* **1981**, *103*, 3702. Wolfe, S.; Mitchell, D. J.; Schlegel, H. B. *J. Am. Chem. Soc.* **1981**, *103*, 7692; **1981**, *103*, 7694. Wolfe, S.; Mitchell, D. J.; Schlegel, H. B. Minot, C.; Eisenstein, O. *Tetrahedron Lett.* **1982**, *23*, 615. Wolfe, S.; Mitchell, D. J.; Schlegel, H. B. *Can. J. Chem.* **1982**, *60*, 1291. Mitchell, D. J.; Schlegel, H. B.; Shaik, S. S.; Wolfe, S. *Can. J. Chem.* **1985**, *63*, 1642.
(25) Wolfe, S. *Can. J. Chem.* **1984**, *62*, 1465. Wolfe, S.; Stolow, A.; La John, L. A. *Can. J. Chem.* **1984**, *62*, 1470.
(26) Dedieu, A.; Veillard, A.; Roos, B. In *Proceedings of the 6th Jerusalem Symposium on Quantum Chemistry and Biochemistry*; D. Reidel: Dordrecht, 1973; p 371.
(27) Dedieu, A.; Veillard, A. In *Reaction Transition States*; Dubois, J. E., Ed.; Gordon and Breach Science Publishers: New York, 1972; p 153.
(28) Keil, F.; Ahlrichs, R. *J. Am. Chem. Soc.* **1976**, *98*, 4787.
(29) Černušák, I.; Urban, M.; Čársky, P.; Treindel, L. *Chem. Zvesti* **1982**, *36*, 749. Urban, M.; Černušák, I.; Kellö, V. *Chem. Phys. Lett.* **1984**, *105*, 625.
(30) Černušák, I.; Diercksen, G. H. F.; Urban, M. *Chem. Phys. Lett.* **1986**, *128*, 538.
(31) Raghavachari, K.; Chandrasekhar, J.; Burnier, R. C. *J. Am. Chem. Soc.* **1984**, *106*, 3124.
(32) Havlas, Z.; Merkel, A.; Kalcher, J.; Janoschek, R.; Zahradník, R. *Chem. Phys.*, in press.
(33) Glasstone, S.; Laidler, K. J.; Eyring, H. *The Theory of Rate Processes*; McGraw-Hill: New York, 1941.
(34) Ryaboy, V. M. *Theor. Exp. Chem. (Engl. Transl.)* **1986**, *217*, 435. Ryaboy, V. M.; Basilevsky, M. V. *Chem. Phys. Lett.* **1986**, *129*, 71.

$$CH_3F + H^- \rightarrow CH_4 + F^- \quad (1)$$

We employed the reaction scheme proposed by Brauman and co-workers.[9,10,35,36]

The S_N2 reaction under consideration is interpreted as a sequence of elementary steps with the corresponding rate constants (cf. Figure 1). Assuming steady-state concentrations of complexes B and D, respectively, the following expression is valid for an overall rate constant k^{obs} which corresponds to the experimental value:[37]

$$k^{obs} = k_{AB}k_{BD}k_{DE}/\{k_{BA}(k_{DB} + k_{DE}) + k_{BD}k_{DE}\} \quad (2)$$

For highly exothermic reactions (for reaction 1 an enthalpy change of $H^{exp} \approx -56$ kcal/mol was found[6]), k_{DB} can be neglected relative to k_{DE} and the expression simplifies to

$$k^{obs} \approx k_{AB}/(1 + k_{BA}/k_{BD}) \quad (3)$$

Thus, knowledge of the initial part of the energy profile (from A to C in Figure 1) is sufficient for evaluation of the rate constant k^{obs}.

The collision of the reactants with rate constant k_{AB} is governed by long-range ion-induced dipole and permanent dipole interactions.

Both decompositions of complex B into the reactants and products are unimolecular steps differing in the character of the corresponding activated complexes. The process B → D possesses a "tight" transition state C‡, located at the maximum C of the potential curve, and the process B → A has a "loose" activated complex BA‡ due to the lack of a barrier on the potential energy surface. The position of the complex BA‡ is located either at the centrifugal maximum[10,38] (model A in our calculations) or according to the generalized transition state theory[39] at the minimum number of internal states along the potential profile (model B in our calculations). Rate constant k_{BA} is larger than k_{BD} (even for an energy difference $\Delta E_{AC} = 0$) owing to the higher number of states for the "loose" transition state BA‡ compared to the "tight" one, C‡.

Evaluation of k_{AB}. The process A → B with rate constant k_{AB} is governed by ion–molecule capture. The long-range potential

$$V(r) = -\alpha_p q^2/r^4 \quad (4)$$

for a charge-induced dipole interaction leads to the expression for the Langevin rate constant[40]

$$k_L = 2\pi q(\alpha_p/\mu)^{1/2} \quad (5)$$

Here r denotes the distance between the center of mass of the ion with charge q and the molecule with polarizability α_p, and μ is the reduced mass. If the molecule has a permanent dipole moment μ_D, the dipole is "locked" into the potential characterized by the expression

$$V(r,\vartheta) = -q\mu_D \cos \vartheta/r^2 \quad (6)$$

taking into account the anharmonicity of the potential. If the angle ϑ between the dipole axis and the line connecting the center of mass is fixed at $\vartheta = 0°$, then an additional rate constant contribution

$$k_D = 2\pi q\mu_D(2/\pi\mu k_B T)^{1/2} \quad (7)$$

is obtained (k_B is the Boltzmann constant). In reality a "locking" constant C, smaller than unity, has been introduced[41] so that the rate constant k_{AB} is given by the expression

$$k_{AB} = k_L + Ck_D \quad (8)$$

Constant C can be evaluated using the relationship proposed by Troe[42] on the basis of the adiabatic channel model[43]

$$C \approx 1 - 0.614 \exp\{-(B'/k_B T)^2\} \quad (9)$$

where B' denotes the rotational constant assuming that complex B is linear.

Evaluation of the Ratio k_{BA}/k_{BD}. Molecules of the B complex are chemically activated species (e.g., energetically excited by the reaction A → B) decomposing either into products (with the rate constant k_{BD}) or back into reactants (k_{BA}). For an arbitrary pressure p (p is proportional to concentration of particles [M]), the general relation is obtained (see ref 11, p 268):

$$\frac{k_{BA}}{k_{BD}} = \frac{\int_0^\infty k_{BA}(E)F(E)/(k_{BD}(E) + k_{BA}(E) + \omega)\,dE}{\int_0^\infty k_{BD}(E)F(E)/(k_{BD}(E) + k_{BA}(E) + \omega)\,dE} \quad (10)$$

$F(E)$ denotes the energy distribution function of chemically activated complex B. Both the specific rate constants $k_{BA}(E)$ and $k_{BD}(E)$ at energy E are evaluated according to the RRKM theory[11]

$$k_{BA}(E) = W_{BA^\ddagger}(E - \Delta E^\ddagger_{BA})/h\rho(E) \quad (11a)$$

$$k_{BD}(E) = W_{C^\ddagger}(E - \Delta E^\ddagger_{BC} - \Delta E_{rot})/h\rho(E) \quad (11b)$$

$W_{BA^\ddagger}$ and $W_{C^\ddagger}$ are the numbers of states at the critical configurations BA‡ and C‡, ρ is the density of states of the complex B, and h is the Planck constant. $\Delta E^\ddagger_{BA}$ and $\Delta E^\ddagger_{BC}$ denote the sum of the potential and ground state vibrational energy values of the critical configurations for the reactions B → A and B → D, respectively. ΔE_{rot} approximates the change of the overall rotation

$$\Delta E_{rot} = k_B T(1 - I_{BD}/I_{BA}) \quad (12)$$

in terms of moments of inertia I_{BD} and I_{BA} of both the activated complexes.

Using the strong collision assumption, we can get the collision frequency ω in the form of product of collision number Z and pressure p (ref 11, p 164):

$$\omega = Zp \quad (13)$$

$$Z = (\sigma_d^2 N_A/R)(8\pi N_A k_B/(\mu T))^{1/2} \quad (14)$$

σ_d is the collision diameter, N_A the Avogadro constant, R the gas constant, T the temperature, and μ the reduced mass.

Followig Olmstead and Brauman,[10] we have taken the distribution function $F(E)$ for this kind of chemical activation in the form:

$$F(E) = \frac{W_{BA^\ddagger}(E - \Delta E^\ddagger_{BA}) \exp(-E/k_B T)}{\int_0^\infty W_{BA^\ddagger}(E - \Delta E^\ddagger_{BA}) \exp(-E/k_B T)\,dE} \quad (15)$$

Although the pressure in the flowing afterglow measurements is typically five orders of magnitude higher than that in the ICR measurements, the assumption $\omega \ll k_{BA}(E)$, $k_{BD}(E)$ is still valid (compare section III). This means that collision deactivation is negligible in comparison with decomposition of complex B. Thus, eq 10 can be simplified:

$$k_{BA}/k_{BD} = \frac{\int_0^\infty \frac{k_{BA}(E)}{k_{BD}(E) + k_{BA}(E)} F(E)\,dE}{\int_0^\infty \frac{k_{BD}(E)}{k_{BD}(E) + k_{BA}(E)} F(E)\,dE} \quad (16)$$

(35) Jasinski, J. M.; Brauman, J. I. *J. Am. Chem. Soc.* **1980**, *102*, 2906.
(36) Pellerite, M. J.; Brauman, J. I. *J. Am. Chem. Soc.* **1980**, *102*, 5993.
(37) Eigen, M. *Angew. Chem., Int. Ed. Engl.* **1964**, *3*, 1.
(38) Waage, E. V.; Rabinovitch, B. S. *Chem. Rev.* **1970**, *70*, 377.
(39) Garrett, B. C.; Truhlar, D. G. *J. Phys. Chem.* **1979**, *83*, 1052.
(40) Langevin, P. M. *Am. Chem. Phys.* **1905**, *5*, 245.
(41) Su, Y.; Bowers, M. T. *J. Chem. Phys.* **1973**, *58*, 3027.
(42) Troe, J. *Chem. Phys. Lett.* **1985**, *122*, 425.
(43) Quack, M.; Troe, J. *Ber. Bunsenges. Phys. Chem.* **1974**, *78*, 240.

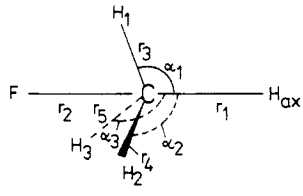

Figure 2. Definition of the internal coordinates for the stationary points A, B, and C.

Table I. Geometries[a] of the Stationary Points of Reaction $CH_3F + H^- \rightarrow CH_4 + F^-$ Completely Optimized at the MP2 Level Using the 6-311G** Basis Set

denotation	r_1	r_2	r_{CH}	α^b	$\beta^{b,c}$
A[d]		1.3816	1.0917	109.20	109.74
B	2.8359	1.4178	1.0872	109.75	109.19
C	1.8166	1.7060	1.0744	96.63	118.69

[a] In Å and deg. For an explanation of the geometry parameters, see Figure 2. [b] $r_{CH} = r_3 = r_4 = r_5$, $\alpha = \alpha_1 = \alpha_2 = \alpha_3$, $\beta = \beta_1 = \beta_2 = \beta_3$. [c] According to the relation: $\sin(\alpha/2) = \sqrt{3}/2 \sin\alpha$. [d] According to: Kondo, S.; Koga, Y.; Nakanaga, T. *J. Chem. Phys.* **1984**, *81*, 1951.

As discussed above, $k_{BA}(E) > k_{BD}(E)$, and therefore the nominator in eq 16 yields

$$\int_0^\infty k_{BA}(E)/(k_{BD}(E) + k_{BA}(E))F(E)\,dE \approx \int_0^\infty F(E)\,dE = 1 \tag{17}$$

Substituting eq 11a and 11b and 17 into eq 16, the final expression for ratio k_{BA}/k_{BD} is obtained (equivalent to that used by Olmstead and Brauman[10]):

$$\frac{k_{BA}}{k_{BD}} = \frac{\int_0^\infty W_{BA^\ddagger}(E - \Delta E^\ddagger_{BA}) \exp(-E/k_BT)\,dE}{\int_0^\infty W_{C^\ddagger}(E - \Delta E^\ddagger_{BC} - \Delta E_{rot}) \exp(-E/k_BT)\,dE} \tag{18}$$

The activated complex for the reaction B → D is fixed at the corresponding transition state of the potential energy surface. Two approaches have been used for finding the critical configurations of the process B → A.

Model A. The critical configuration is located at the maximum of the sum of the potential and centrifugal energies as described in ref 38. The two vibrational modes (with frequencies ω_7, Table II) corresponding to free rotations of the separated fragments are treated as free internal rotors. This procedure was used previously by Olmstead and Brauman.[10]

Model B. The critical configurations were located at the point on the reaction path corresponding to the minimum number of states for the internal degrees of freedom according to generalized transition-state theory.[39] The minimum number of states is calculated for a specific energy E; it means the critical configuration is energy dependent. The two vibrational modes which correlate with free rotations of fragments are treated as vibrations with decreasing frequency values ω_i. The decrease of these frequency values along the reaction path can be described by a semiempirical relation[44]

$$\omega_i(r_{CH_{ax}}) = \omega_i(r^B_{CH_{ax}}) \exp\{-\alpha(r_{CH_{ax}} - r^B_{CH_{ax}})\} \tag{19}$$

where $r^B_{CH_{ax}}$ is the equilibrium distance r_2 (see Figure 2) in complex B and $r_{CH_{ax}}$ is the distance of the C and H_{ax} atoms, which varies along the reaction path of process B → A. (Therefore an approximate reaction path has to be constructed.) There is no straightforward way to evaluate parameter α in eq 19. The value used in this work is based on literature data for reactions possessing "loose" transition states. Troe[45] suggested a relation between parameter α and parameter β in the Morse function, namely, $\alpha/\beta \approx 0.5$ (for β, vide infra). According to Quack[46] a value of $\alpha =$ 1.0 Å^{-1} can be employed for a wide variety of complex formation reactions.

Table II. Vibrational Frequencies[a] (ω^i), Zero-Point Energies[b] (E_{ZP}), and Moments of Inertia[c] (I_A, I_B, I_C) for Stationary Points A, B, and C (see Figure 1)

	A	B	C
ω_1	3116.9 (1)	3167.6 (1)	3227.0 (1)
ω_2		464.0 (1)	730.6 (1)
ω_3	1105.7 (1)	978.7 (1)	i975.5 (1)
ω_4	1614.0 (1)	1511.1 (1)	1355.5 (1)
ω_5	3189.3 (2)	3267.4 (2)	3459.9 (2)
ω_6	1598.7 (2)	1579.8 (2)	1482.1 (2)
ω_7		190.6 (2)	490.1 (2)
ω_8	1267.4 (2)	1211.5 (2)	1170.9 (2)
E_{ZP}	25.66	26.62	26.47
I_A	3.2142	3.1731	3.4445
I_B, I_C	19.6513	33.1580	34.3444

[a] In cm^{-1}. [b] In kcal mol^{-1}. [c] In amu Å^2.

Table III. Relative Energy Data Sets Used for Calculations of the Rate Constant of the Reaction $CH_3F + H^- \rightarrow CH_4 + F^-$

no. of data set	method[a]	ΔE (kcal mol^{-1}) A	B	C
I	MP2/6-311G**//MP2/6-311G**	0	−12.02	1.38
II	MP2/6-311++G**//MP2/6-311G**	0	−8.42	1.11
III	MCSCF-CI+D/DZP//MP2/6-311G**	0	−7.92	3.83
IV	MP4(SDTQR)/DZP	0	−7.8[b]	2.0

[a] Methods and basis sets are explained in ref 32 (I–III) or in ref 29 (IV). [b] Value taken from ref 34.

Table IV. Experimental Quantities and Derived Values Used for the Evaluation of Rate Constants k_{AB} and k_{BA}

properties	symbol	value
polarizability of CH_3F (au)	α_p	17.62[a]
dipole moment of CH_3F (au)	μ_D	0.728[b]
parameter of Morse function (Å^{-1})	β	0.70
parameter of frequency change (Å^{-1})	α	0.35
dipole "locking" constant	c	0.3875
moments of inertia for activated complex B → A (model A), symmetry number (amu Å^2)	I_i; σ_i	75.0; 3(2)[c]

[a] Reference 47. [b] Reference 48. [c] Degeneracy in parentheses.

III. Details of Calculations

Geometry parameters and frequency values used for the evaluation of the rate constants are summarized in Tables I and II (for definitions, see Figure 2). Rate constant calculations were performed for four different sets of energy data. Three of them (I–III in Table III) are the results of quantum chemical calculations.[32] Only beyond Hartree–Fock energies, including the correlation energy, were used. Data set IV was taken from the paper by Ryaboy[34] in which two-dimensional scattering calculations were performed and allowed for comparisons with our statistical results. The other data used in this work are summarized in Table IV. The polarizability and dipole moment of CH_3F were taken from experimental data[47,48] because no reliable quantum chemical results were available.

The rate cosntants k_{BA}, and k_{BD} were calculated according to the RRKM theory using a modified version of the program of Hase and Bunker[51]. The number and densities of vibrational states were evaluated by a direct counting procedure and the internal rotational states were treated classically. The integration of the eq 18 was performed numerically.

For model A the maximum of the centrifugal barrier was located at a distance of 7.4 Å. The corresponding moments of inertia for the activated complex and the degeneracy factors are summarized in Table IV.

(44) Johnston, H. S. *Gas Phase Reaction Rate Theory*; Ronald Press: New York, 1966.
(45) Troe, J. *J. Chem. Phys.* **1981**, *75*, 226.
(46) Quack, M. *J. Phys. Chem.* **1979**, *83*, 150.
(47) Nelson, R. D.; Lide, D. R. NBS NSRDS 10; U.S. Government Printing Office: Washington, DC; 1097.
(48) Bogaard, M. P.; Buckingham, A. D.; Piersen, R. K.; White, A. H. *J. Chem. Soc., Faraday Trans. 1* **1973**, *74*, 3008.

Table V. Calculated Reaction Rate[a] k_{obs} and Efficiency of the Reaction $CH_3F + H^- \rightarrow CH_4 + F^-$ at $T = 300$ K

	k_{obs} ($cm^3\ s^{-1}$)		efficiency	
data set[b]	model A	model B	model A	model B
I	2.5×10^{-11}	6.7×10^{-12}	0.0024	0.0006
II	4.5×10^{-11}	1.6×10^{-11}	0.0043	0.0015
III	2.1×10^{-12}	2.0×10^{-13}	0.0002	0.00002
IV	1.5×10^{-11}	4.1×10^{-12}	0.0014	0.0004
exp[c]	1.5×10^{-11}		0.0020	

[a] Calculated rate constant k_{AB} used in eq 3 has value 1.0×10^{-8} $cm^3\ s^{-1}$. [b] For definition, see Table III. [c] Reference 6, $k_{AB} = 7.6 \times 10^{-9}$ $cm^3\ s^{-1}$.

To perform calculations according to model B, an "intuitive" reaction path was defined. We started at the equilibrium geometry of complex B with the following assumptions: (1) At a distance $r_{CH_{ax}} = 6$ Å the product geometry of CH_3F is reached. (2) The change between the geometry parameters of the B complex and that of the product, CH_3F, is a linear function of $r_{CH_{ax}}$. Quantum chemical calculations were performed for five points on the intuitive reaction path using the second-order Møller–Plesset perturbation theory[49] (MP2) with the 6-311G** basis set.[50] The curve constructed from these points was compared with the semiempirical potential curve (eq 4 and 6). A Morse function (20) was fitted to the potential function:

$$V(r_{CH_{ax}}) = D\{1 - \exp(-\beta(r_{CH_{ax}} - r^{B}_{CH_{ax}})\}^2 \qquad (20)$$

to estimate the value of parameter β and subsequently parameter α according to Troe's relation, mentioned above. An average value of parameter $\beta = 0.70$ $Å^{-1}$ was found, yielding $\alpha = 0.35$ $Å^{-1}$. When using a value of $\alpha = 1.0$ $Å^{-1}$, no minimum in the number of states was found owing to the steep decrease in the frequency values.

A rough estimate of collision frequency ω according to eq 13 and 14 leads to a value of $\omega = 10^8$ s^{-1} assuming collision diameter $\sigma_d \approx 30$ Å and pressure of 0.2 Torr. The minimum values of specific rate constants $k_{BA}(E)$ and $k_{BD}(E)$ occur at energies just above that of the barrier or the critical configuration. The minimum of the specific rate constants $k_{BD}(E)$ is smaller than $k_{BA}(E)$ owing to the higher energy of C compared to the energy of reactants A (see Table III). The rate constant $k_{BD}(E)$ is about 10^{10} s^{-1}, which means that the collision frequency ω is always at least two orders of magnitude smaller than $k_{BD}(E)$ (and, of course, $k_{BA}(E)$). Therefore the approximations used in eq 18 seem to be valid.

IV. Results and Discussions

The evaluated rate constants k_{obs} and corresponding efficiencies (efficiency = k_{obs}/k_{AB}) at 300 K are summarized in Table V. For data sets I–IV, the rate constants differ by less than half an order of magnitude depending on the model used. The smaller values of k_{obs} calculated for model B in comparison with model A are the consequence of larger values of k_{BA} in model B.

As far as we know, the only experimental value available for this reaction is that obtained by the flowing afterglow measurement of Tanaka et al.[6] ($k^{exp}_{obs} = 1.5 \times 10^{-11}$ $cm^3\ s^{-1}$, $T = 300$ K). We found good agreement between the results obtained using data sets I, II, and IV and the experimental value. The rate constant k_{obs} calculated with data set III is at least one order of magnitude smaller owing to the rather large reaction barrier predicted by the MCSCF–CI calculations ($E_{AC} = 3.8$ kcal/mol). Differences in the depth of minimum B have smaller influence (compare I and II) because the ratio k_{BA}/k_{BD} is almost constant although the absolute values differ appreciably. Surprisingly, we also found good agreement between the results obtained using data set IV (1.5×10^{-11} and 4.1×10^{-12} $cm^3\ s^{-1}$) and the results of the scattering calculations[33] (1.1×10^{-11} $cm^3\ s^{-1}$) although both approaches are based on completely different (if not mutually exclusive) kinetic assumptions.

The experimentally estimated barrier value[6] of 3.7 kcal/mol requires comment. It was estimated using the Arrhenius equation at a single temperature and without taking into account the ratio of the partition functions for the internal degrees of freedom of reactant A and transition state C. If the reaction is treated as a direct process according to the Eyring theory[33] and using the values of the calculated barrier heights (cf. Table III), the values for k_{obs} are much smaller than the experimental rate constant (7.0×10^{-13}, 7.6×10^{-13}, 1.9×10^{-15}, 1.7×10^{-13} $cm^3\ s^{-1}$ for data sets I–IV, respectively.) Therefore, the experimental barrier value has to be accepted with caution.

Finally, barrier heights of 1 to 2 kcal/mol allow us to reproduce the available experimental value while higher barrier values lead to rate constants smaller than that measured by employing the statistical treatment proposed by Brauman and co-workers.[9,10,12–14,35,36] Nevertheless, more experimental data seem to be necessary as well as further, more sophisticated quantum chemical calculations, in order to reach final conclusions on the mechanism, rate constants, and dynamics of this simple S_N2 reaction.

Registry No. CH_3F, 593-53-3; H^-, 12184-88-2.

(49) Møller, C.; Plesset, M. S. *Phys. Rev.* **1934**, *46*, 618.
(50) Krishnan, R.; Binkley, J. S.; Seeger, R.; Pople, J. A. *J. Chem. Phys.* **1980**, *72*, 650.
(51) Hase, W. L.; Bunker, C. L. Quantum Chemistry Program Exchange, No. 234, Indiana University.